Int. J. Electrochem. Sci., 14 **(2019)** 10888 – 10906, doi: 10.20964/2019.12.05

International Journal of
ELECTROCHEMICAL
SCIENCE
www.electrochemsci.org

Experimental Data Treatment of the Pipeline Steel Polarization Curve under AC Interference

Shouxin Zhang[1], *Zili Li*[1,*], *Xinyi Su*[2], *Chao Yang*[1]

[1] College of Pipeline and Civil Engineering, China University of Petroleum, No. 66, Changjiang West Road, Huangdao District. Qingdao 266580, China
[2] CNOOC Energy Development Equipment Technology Co., No. 867, Huayuan Industrial Zone. Tianjin 300450, China
[*]E-mail: zilimenhuzu@163.com

Received: 13 June 2019 / *Accepted:* 16 August 2019 / *Published:* 29 October 2019

The treatment of polarization curves of pipeline steels subject to AC (Alternating Current) was studied. The Tafel exploration, the non-linear curve fitting method, and the SYMADEC (synthesis, matching, and deconvolution of polarization curves) algorithm were used to evaluate the Tafel slopes and the corrosion current density from a set of experimental polarization curves. The results of the Tafel exploration show a large variation when different linear portions were selected for the calculation. The non-linear curve fitting method is sensitive to noise and easy to fail when used to fit planarization data presenting AC signal. SYMADEC is a robust method to fit the experimental polarization curves, which do not present a Tafel region. Moreover, the results of SYMADEC can be deconstructed into the anodic and cathodic components providing more kinetics information about the electrode process. Therefore, in the study of the AC corrosion behavior by polarization curves exhibiting no Tafel region, the experimental data should be carefully treated to obtain accurate values of the kinetics parameters. The use of SYMADEC is recommended in this case.

Keywords: polarization curve; Tafel slope; corrosion current; AC corrosion

1. INTRODUCTION

The measurement of polarization curves is a basic electrochemical technique in the study of corrosion processes. It can be used to evaluate corrosion kinetics parameters, such as the anodic and cathodic Tafel slopes and the corrosion current density.[1] Moreover, the passivity behavior of metals and alloys can be studied via the anodic branch of the polarization curve, since several passivity parameters such as the passivation potential and current density can be determined.[2, 3] Moreover, in

the study of the pitting phenomena on metal surfaces, the breakdown and the re-passivation potential can also be measured from the polarization curves. [4-6]

In the study of the AC corrosion behavior, testing the polarization curve is a well-used method to reveal the electrochemical mechanism behind this process. In a series of studies performed by Chin and coworkers, the effects of AC on the passive behavior of different metals were examined by measuring their anodic polarization. Their results showed that the influence of the AC on the passivity process of carbon steel was similar to that of chloride ions.[7-13] By testing the polarization curves of different metallic materials in different solutions under the effect of the AC, Goidanich et al. discussed the effects of the AC interference on the corrosion kinetics parameters of the samples.[14] Cheng et al. analyzed the relation between the anodic current density and the shift of the corrosion potential for various AC densities by using potentiodynamic polarization curve measurements.[15] Wang et al. evaluated the kinetics parameters of X70 and X80 steel in simulated soil solutions under the influence of different AC densities by fitting the polarization curves, and confirmed that AC may have an impact both on the anodic and on the cathodic process.[16]

Although the polarization curve is a classic way to evaluate the kinetics parameters characteristic of the metal corrosion process[17], it is based on the extrapolation of the Tafel curve, which requires that at least one of the anodic or cathodic branches exhibits a Tafelian behavior in the strong polarization region about the 50–100 mV range away from the corrosion potential.[18] A typical polarization curve showed in the textbooks to explain the Tafel method is in an ideal situation: it has an obvious linear part, which is easy to extrapolate to obtain the values of the kinetics parameters. Unfortunately, the polarization curves obtained in a laboratory are effected by many factors, which induce a complicated shape in the actual curve, and lead to erroneous conclusions when the Tafel extrapolation method is applied. Several commercial software are designed for specific electrochemical instruments and apply the non-linear least squares fitting method to the polarization curve to improve the accuracy of the results. [18] However, due to the complicated non-Tafel behavior of the experimental curve, the algorithms may not be robust enough and can easily produce questionable results. In order to improve the accuracy of the polarization curve analysis, several methods have been developed. [17, 19-25]

AC plays a unique role when compared to other factors that influence the corrosion process, such as temperature, ion concentration, or pH. Essentially, AC is an electrical signal and it is same with the driving force introduced by any potentiostat or electrochemical workstation during the polarization test process. Therefore, when AC is applied to a system via an external power source, it generates unavoidable interferences with the performance of the test instruments, inducing alternating noise in the polarization data. When the interferences are large enough compared to the polarization potential, the test process may break down. Moreover, the applied AC may reinforce the non-Tafel behavior of the polarization curve, which becomes more challenging to analyze. However, the kinetics parameters estimated from the polarization curve are fundamental to investigate the AC corrosion mechanism. For example, the shift of the corrosion potential induced by the AC was erroneously associated to the ratio between the anodic and the cathodic Tafel slopes.[26-29]Therefore, the accuracy of the analysis of the polarization curve is essential. However, the treating process of the polarization curve under AC interference has not been studied in the published papers yet.

In this paper, the treatment of the pipeline steel polarization curves under the effect of AC was studied. Three methods, the Tafel exploration, the non-linear curve fitting method, and SYMADEC, were used to evaluate the kinetics parameters of the corrosion process from the polarization curves, and the validity of the three methods was discussed. This work provides an instruction to guide future research in obtaining more accurate and meaningful information from the polarization curves in the study of AC corrosion.

2. EXPERIMENT AND METHOD

2.1 Materials and solutions

In this paper, two sets of polarization data were used for the treatment. The first one (Case I) was extracted from the polarization curves, which have been previously published in literature[15]. The second one (Case II) originated from a series of polarization test experiments performed in the laboratory of the authors of this paper.

The preparation process of the electrodes used in both Case I and II was identical and it was previously described in Ref.[15]. Initially, the steel samples were cut into areas of size 10 × 10 × 3 mm, then they were carefully embedded in epoxy resin with a wire soldered at the back. When the epoxy resin completely solidified, the working side of the electrode was subsequently grounded with a series of sand papers, and then was carefully cleaned with distilled water and methanol to obtain a homogeneous surface.

The chemical composition of the pipeline steels and the solutions used in the two cases are listed in Table 1 and Table 2.

Table 1. Chemical composition of the pipeline steels

Case I (16Mn)													
Element	C	Mn	S	P	Si	Cr	Mo	Al	V	Ti	Cu		
Content(wt.%)	0.16	1.4	0.025	0.009	0..36	<0.1	<0.05	<0.03	<0.03	<0.03	<0.055		
Case II (X90)													
Element	C	Si	Mn	P	S	Ni	Cr	Cu	Nb	Ti	Mo	Al	B
Content(wt.%)	0.057	0.18	1.85	0.008	0.001	0.18	0.19	0.15	0.054	0.011	0.16	0.03	0.0004

Table 2. Chemical composition of the solutions

Case I			
Reagent	KCl	$MgSO_4 \cdot 7H_2O$	$NaHCO_3$
Content(g/L))	8.933	1.17	5.51
Case II			
Reagent	Na_2SO_4		
Content(mol/L)	0.1		

2.2 Polarization curve test under AC

Despite traditional three electrodes systems, consisting of a working electrode, a counter electrode, and a reference, are normally used to carry out AC polarization tests, the circuit has to be carefully designed to minimize the interferences between the AC power and the test instrument. The schematic diagram of a typical AC polarization setup is shown in Fig. 1. Two circuit loops are present in the diagram: one sets the AC and the other is used to implement the polarization test. A capacitor was used to block the DC to enter the AC loop, and an inductor was used to block the AC to enter DC loop.[30] As a result, the circuit allowed the electrochemical workstation to control the DC potential of the working electrode and to measure the polarization current with the permitting AC passing through the electrode. The value of the capacitor and of the inductance used in the experiment are 1000 μF and 10 H. In order to decrease the influence of the ohmic drop on the potential measurement, the reference electrode was immerged in a Luggin capillary and positioned 2 mm away from the electrode surface. The parameters used for the polarization test for both Case I and II are listed in Table 3.

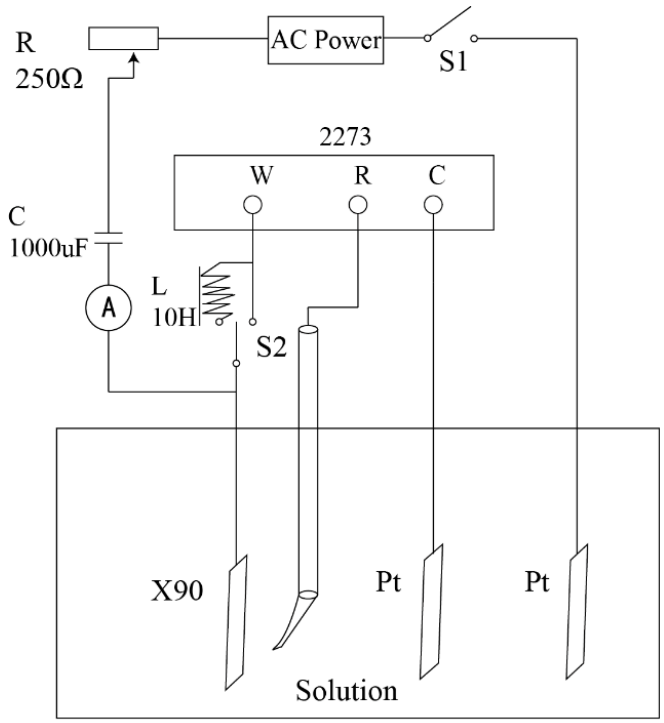

Figure 1. Schematic diagram of the experimental setup for polarization curve test under AC

Table 3. The parameters of polarization tests

	Scanning rate(mV/s)	Potential range(mV)
Case I	0.3	-1500～0(SCE)
Case II	0.166	-250～+250 (vs OCP)

2.3 Analysis methods for polarization curve

Three methods, the Tafel extrapolation, the non-linear curve fitting method, and the method proposed in Ref.[21] known as SYMADEC, were used to analyze the polarization curves tested in the presence of AC. The theoretical basis of the three methods is the Wagner-Traud equation[31]:

$$I = I_{\text{corr}}\left[\exp\left(2.303\frac{E-E_{\text{corr}}}{\beta_{\text{a}}}\right)-\exp\left(-2.303\frac{E-E_{\text{corr}}}{\beta_{\text{c}}}\right)\right] \quad (1)$$

where I is the applied current density, I_{corr} is the corrosion current density, E is the applied potential, E_{corr} is corrosion potential, and β_{a} and β_{c} correspond to the anodic and the cathodic Tafel slope, respectively.

2.3.1 Tafel extrapolation

Tafel extrapolation is a well-known method. When the value of the applied potential is far enough away from the corrosion potential, the polarization curve only reflects the kinetics information of one electrode process in the anodic or cathodic branch. Therefore, the linear parts of the polarization curve can be extrapolated into an intersection, which provides the values of E_{corr} and I_{corr}. The slopes of the anodic and cathodic linear portions are defined as β_{a} and β_{c}, respectively. The Tafel extrapolation is easy to perform; however, it is error-prone, since the linear portions may not be obvious due to the noise and errors introduced during the experiment. To obtain an accurate result, two rules were defined in Ref.[18]: (a) the linear trend should be observed in at least one of the two branches over a range of one decade of the current density plotted in a semilogarithmic scale, and (b) the potential of the initial points of the extrapolation should be higher than 50–100 mV when compared to E_{corr}.

2.3.2 Nonlinear curve fitting method

If the potential is larger than that required one in linear polarization, but it is still too small for Tafel extrapolation, the polarization curve is the synthesis of the anodic and cathodic electrode process. Several approaches have been proposed to compute β_{a}, β_{c}, and I_{corr} from this range of polarization curve, such as the three point method[32] and the four point method[33]. By using these methods, the influence of the large potential in the Tafel extrapolation region and the error generated over the approximation process in linear polarization region can be avoided. Furthermore, with the development of novel computer techniques, the non-linear curve fitting method has been applied in the processing of polarization data in such specific potential region. The principle of the non-linear curve fitting method is based on adjusting the undetermined parameters to minimize the difference between the calculated and the experimental values. However, the use of the non-linear curve fitting method to fit the experimental curve requires technical mathematic and programming abilities. Fortunately, such complex non-linear curve fitting techniques have been packaged in several software, such as Origin and Matlab, which are currently widely used in scientific research.

In this paper, the non-linear curve fitting function developed in Origin was used as non-linear curve fitting tool. Although the fitting process can be easily implemented with the help of a data

processing software, the selection of the initial values is still an important issue. If the initial values diverge too much from the true ones, the fitting process may fail. Therefore, in practice the successful fitting is based on experience. Moreover, when the target equation becomes complicated, the fitting process becomes more difficult to be convergent.

2.3.3 SYMADEC

In order to fit the experimental polarization curve for the $Fe/H_2O/H^+/O_2$ corrosion system, Flitt and Schweinsberg[17, 21] developed a non-commercial computer algorithm, known as SYMADEC. One important feature of SYMADEC is that after the computation is completed, the fitted curve can be deconstructed into two curves, the true anodic and cathodic polarization curves, which provide more information about the corrosion process. The experimental results presented in Ref. [21] demonstrate that SYMADEC accurately fits the polarization curves, which exhibit a non-Tafel region. Here, the use of SYMADEC for the fitting of polarization curves without a passive region is briefly introduced.

The cathodic overpotential of the cathodic reaction, $\eta_{act,c}$, under activation control is expressed as follows:

$$\eta_{act,c} = -\beta_c \log\left(\frac{I_c}{I_{0,c}}\right) \qquad (2)$$

where I_c is the cathodic current density, $I_{0,c}$ is the cathodic exchange current density.

Under the completed concentration polarization, the expression of the overpotential of the concentration, $\eta_{conc,c}$, is expressed as follows:

$$\eta_{conc,c} = \frac{2.303RT}{nF}\log\left(1-\frac{I_c}{I_L}\right) \qquad (3)$$

where n is the number of electrons involved in the reaction, F = 96494 C is the Faraday's constant, R = 8.314 $JK^{-1}mol^{-1}$ is the ideal gas constant, and I_L is the limiting current density.

The total cathodic potential $\eta_{total,c}$ corresponds to the sum of $\eta_{act,c}$ and $\eta_{conc,c}$, which gives:

$$\eta_{total,c} = \eta_{act,c} + \eta_{conc,c} \qquad (4)$$

After derivation, the expression of the cathodic current density can be approximate to

$$I_{total,c} = \frac{I_{0,c}\exp\left(\frac{2.303\eta_{total,c}}{\beta_c}\right)}{1+\frac{I_{0,c}}{I_L}\exp\left(\frac{2.303\eta_{total,c}}{\beta_c}\right)} \qquad (5)$$

The anodic current density is expressed as

$$I_a = I_{0,a}\exp\left(\frac{2.303\eta_{act,a}}{\beta_a}\right) \qquad (6)$$

where $I_{0,a}$ is the anodic exchange current density and $\eta_{act,a}$ is the anodic overpotential of the charge transfer.

During the polarization curve measurement, the non-passive corrosion product layer may form on the surface of the working electrode. The resistance, R_Ω, of such layer may generate a resistance

polarization, which may lead to the "bending" of the Tafel linear trend. This implies that the electrode potential (E) is larger than the true value (E_{true}) when a current, I, flows across the product layer.

$$E_{true} = E - IR_{\Omega} \quad (7)$$

The general procedure of SYMADEC is based on the use of Eq. (5) and Eq. (6), which are the approximate true cathodic and anodic polarization curves, and are then combined together to form a total curve. The trend of the total curve is continuously modified by adjusting the values of the input parameters, until the calculated curve fits well with the experimental polarization one.

3. RESULTS AND DISCUSSION

3.1 The polarization curves in Case I and II

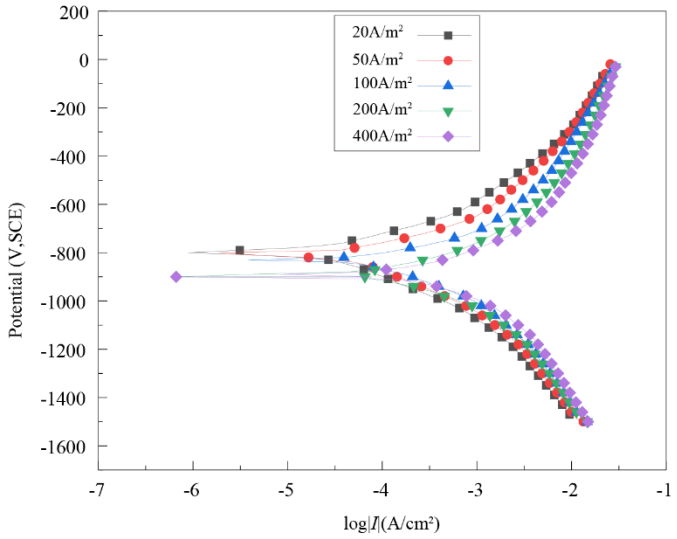

Figure 2. Polarization curves in Cases I measured at various AC current densities

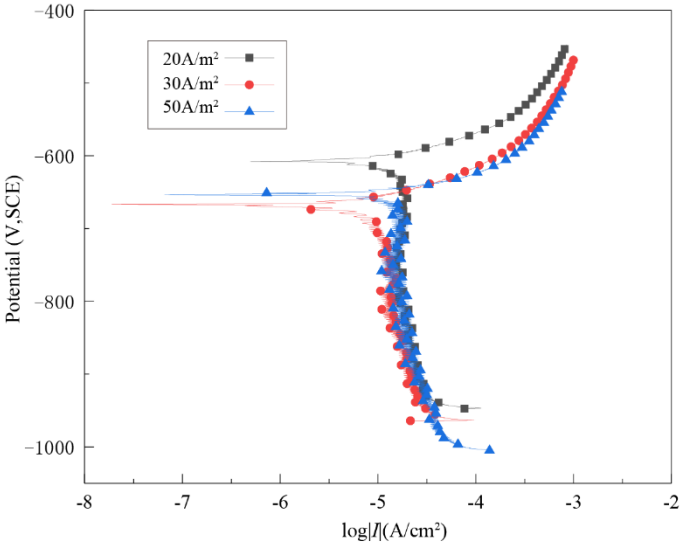

Figure 3. Polarization curves in Cases II measured at various AC current densities

The polarization curves of Case I and II with different AC densities are presented in Fig. 2 and Fig. 3, respectively. The cathodic polarization process, which occurs in Case I was mainly under activation control, while in Case II it was controlled by diffusion. Fig. 3 shows that the actual polarization curves are dramatically influenced by the AC. The kinetics parameters of Cases I, which were obtained by using the commercial software CView 3.2c [15], are listed in Table 4.

Table 4. Kinetics parameters from the polarization curves in Cases I

i_{AC} (A/m^2)	E_{corr} (mV,SCE)	I_{corr} (A/cm^2)	β_a (mV/decade)	β_c (mV/decade)	β_a/β_c
20	-798	2.00×10^{-5}	111	142	0.77
50	-811	4.84×10^{-5}	118	182	0.65
100	-834	9.05×10^{-5}	123	161	0.76
200	-889	1.34×10^{-4}	149	158	0.94
400	-887	2.66×10^{-4}	181	182	0.99

3.2 The results of different methods

3.2.1 Tafel extrapolation

Despite the polarization curves often exhibit non-Tafel portion, due to the easily implement, the Tafel extrapolation has been widely used for the analysis of the polarization curves in the corrosion studies.[2, 34, 35] To verify the effectiveness of this method, the polarization curves of Case I and II were reprocessed by using the Tafel extrapolation method. The results are shown in Table 5 and Table 6.

Table 5. The results of Tafel extrapolation for Case I

i_{AC} (A/m^2)	E_{corr} (mV,SCE)	I_{corr} (A/cm^2)	β_a (mV/decade)	β_c (mV/decade)	β_a/β_c
20	-799	5.21×10^{-5}	151	211	0.72
50	-809	1.14×10^{-4}	166	253	0.66
100	-832	1.37×10^{-4}	136	197	0.69
200	-898	2.56×10^{-4}	212	216	0.98
400	-893	5.06×10^{-4}	248	278	0.89

Table 6. The results of Tafel extrapolation for Case II

i_{AC} (A/m^2)	E_{corr} (mV,SCE)	I_{corr} (A/cm^2)	β_a (mV/decade)	β_c (mV/decade)	β_a/β_c
20	-607	1.74×10^{-5}	46	1407	0.033
30	-668	1.12×10^{-5}	55	1066	0.052
50	-657	1.62×10^{-5}	42	811	0.052

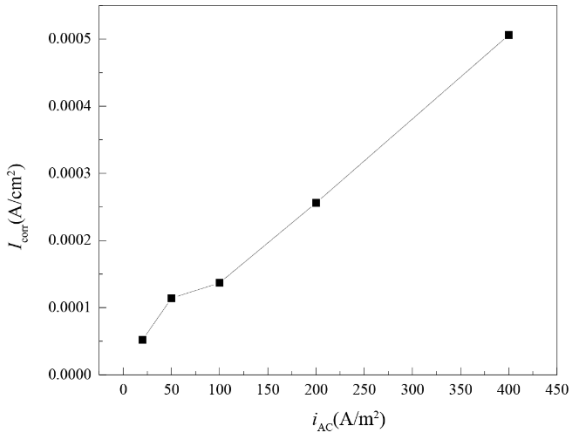

Figure 4. The relation between AC density and the corrosion current evaluated by Tafel extrapolation of Case I

The results of the Tafel extrapolation (Table 5) are not consistent with the results presented in Ref. [15]. Moreover, most of the results of I_{corr}, β_a, and β_c obtained by the Tafel extrapolation are higher than those presented in Ref. [15]. However, as shown in Fig. 4, the I_{corr} value increases when the AC is applied to the system as in Ref. [15].

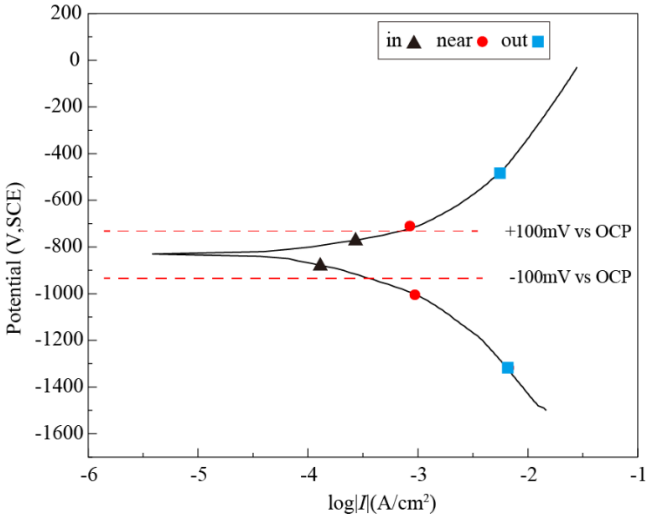

Figure 5. The different positions selected as the linear part for Tafel exploration

As shown in Table 6, the difference between β_a and β_c when an AC density of 20, 30, and 50 A/m^2 is applied is large but the I_{corr} value is similar. This is due to the cathodic polarization process of Case II , which takes place under diffusion control while the anodic polarization process under activation control within the experimental conditions. Therefore, β_c is higher than β_a and this reveals that the corrosion rate is mostly controlled by the diffusion process and not by the AC. As a result, the values of I_{corr} does not vary too much upon an increase in the AC current.[36]

Due to the non-Tafel behavior of the polarization curves, the linear portions may not present obviously. Therefore, the determination of the position of the linear parts in the curves is essential to obtain accurate results. In order to analyze the effect of the different positions of the linear parts on the results, the Tafel extrapolation was performed on three different points, which are suspected to be the critical. The experiment was conducted on the polarization curves of 16 Mn steel in a simulated soil solution under an AC density of 100 A/m^2. The points selected are located in, near, and out of the position that was ±100mV away from the corrosion potential, as shown in Fig. 5. The results of I_{corr}, E_{corr}, β_a, and β_c are listed in Table 7 and they vary for each measured position. When the points are located in a ±100 mV window around the corrosion potential, the estimated values of the kinetics parameters are close to the results presented in Ref. [15]. Otherwise, the results show significant deviations when compared to Ref. [15].When the exploration points are sampled in a range of ±100 mV around the corrosion potential, each branch of the polarization curve contains both the anodic and cathodic information. In the opposite situation and under a large polarization potential, the resistance of the corrosion product "bends" the polarization curve, increasing the error on the experimental result. Therefore, the selection of the linear portion in the polarization curve is of utmost importance to obtain an accurate result when the Tafel extrapolation is used.

Table 7. The kinetics parameters evaluated at different positions in the polarization curve

Position	E_{corr} (mV,SCE)	I_{corr} (A/cm^2)	β_a (mV/decade)	β_c (mV/decade)	β_a /β_c
in	-828	4.20×10^{-5}	72	105	0.69
near	-832	1.37×10^{-4}	136	197	0.69
out	-831	9.57×10^{-4}	456	579	0.79

3.2.2 Nonlinear curve fitting method

The results of the kinetics parameters calculated from the polarization curve of the Case I via the non-linear curve fitting method are listed in Table 8.

Table 8. The results of nonlinear curve fitting method for Case I

i_{AC} (A/m^2)	E_{corr} (mV,SCE)	I_{corr} (A/cm^2)	β_a (mV/decade)	β_c (mV/decade)	β_a /β_c
20	-800	1.34×10^{-5}	84	88	0.95
50	-810	3.70×10^{-5}	106	121	0.88
100	-830	4.00×10^{-4}	289	6.30×10^{23}	4.60×10^{-22}
200	-900	2.91×10^{-4}	4.44×10^{22}	174	2.56×10^{20}
400	-900	4.20×10^{-4}	7.11×10^{22}	150	4.75×10^{20}

Such results are not consistent with Ref. [15]. Moreover, as shown in Table 8, the robustness of the non-linear curve fitting method is poor, as some unreasonable large values are obtained in the results, indicating the failure of such fitting process. The results of Case II are not presented here, since the fitting process failed due to the vibrations present in the polarization curves.

Several factors may influence the fitting results and the most important one is the potential range, which is selected for the fitting process. If this range is too small, the results are sensitive to the errors that may be produced during the test procedure. Otherwise, if the range is too large, some unexpected polarizations, such as resistance polarization caused by the formation of product layer, may be included in the calculation, causing the failure of the model.

In order to analyze the effect of the potential range on the results of the non-linear curve fitting method, a series of intervals (±50 mV, ±100 mV, ±150 mV, and ±200 mV) were used to fit the polarization curves. The results are presented in Table 9. As the potential range increases, more accurate results are obtained via the non-linear curve fitting method. However, the fitting results vary upon a change in the potential range, indicating the presence of unexpected polarizations.

Table 9. The effect of the potential range on the result of the nonlinear curve fitting method

i_{AC} (A/m^2)	ΔE (mV,SCE)	E_{corr} (mV,SCE)	I_{corr} (A/cm^2)	β_a (mV/decade)	β_c (mV/decade)	β_a/β_c
20	±50mV	-800	1.34×10^{-5}	84	88	0.95
	±100mV	-800	2.16×10^{-5}	113	142	0.80
	±150mV	-800	2.31×10^{-5}	114	155	0.74
	±200mV	-800	4.46×10^{-5}	153	206	0.74
50	±50mV	-810	3.70×10^{-5}	106	121	0.88
	±100mV	-810	4.18×10^{-5}	108	159	0.68
	±150mV	-810	5.58×10^{-5}	126	191	0.66
	±200mV	-810	1.03×10^{-4}	170	259	0.66
100	±50mV	-830	4.00×10^{-4}	289	6.30×10^{23}	4.60×10^{22}
	±100mV	-830	8.59×10^{-5}	106	167	0.63
	±150mV	-830	1.61×10^{-4}	154	245	0.63
	±200mV	-830	2.53×10^{-4}	207	303	0.68
200	±50mV	-900	2.91×10^{-4}	4.44×10^{22}	174	2.56×10^{20}
	±100mV	-900	1.14×10^{-4}	152	127	1.20
	±150mV	-900	1.56×10^{-4}	175	160	1.10
	±200mV	-900	2.42×10^{-4}	222	214	1.04
400	±50mV	-900	4.20×10^{-4}	7.11×10^{22}	150	4.75×10^{20}
	±100mV	-900	2.53×10^{-4}	206	147	1.40
	±150mV	-900	3.13×10^{-4}	212	183	1.16
	±200mV	-900	4.08×10^{-4}	236	231	1.02

Therefore, in theory, the nonlinear curve fitting method is useful. However, when it comes to its application in practice, the method is vulnerable to data errors. Hence, it may not be suitable to deal with the polarization curve under the effect of the AC, which could introduce inferences to the test system.

3.2.3 SYMADEC

In order to calculate the value of E_{rev} in anodic and cathodic reactions, several parameters, such as the concentration of O_2 and Fe^{2+} in the solution, as well as its pH and temperature, should be measured initially. Since the solutions used in the two cases were exposed to air, the concentration of O_2 was set to 8 mg/L, and the concentration of Fe^{2+} was set to 0.056 mg/L, a critical value indicating the dissolution of iron in solution. The pH of the solution used in Case I is 8.95, whereas it measures 7.86 in Case II. The temperature was set to 296 K in both cases.

The fitting results of Case I and the anodic and cathodic components obtained via SYMADEC are shown in Fig. 6 and Fig. 7. The estimated kinetics parameters are listed in Table 10.

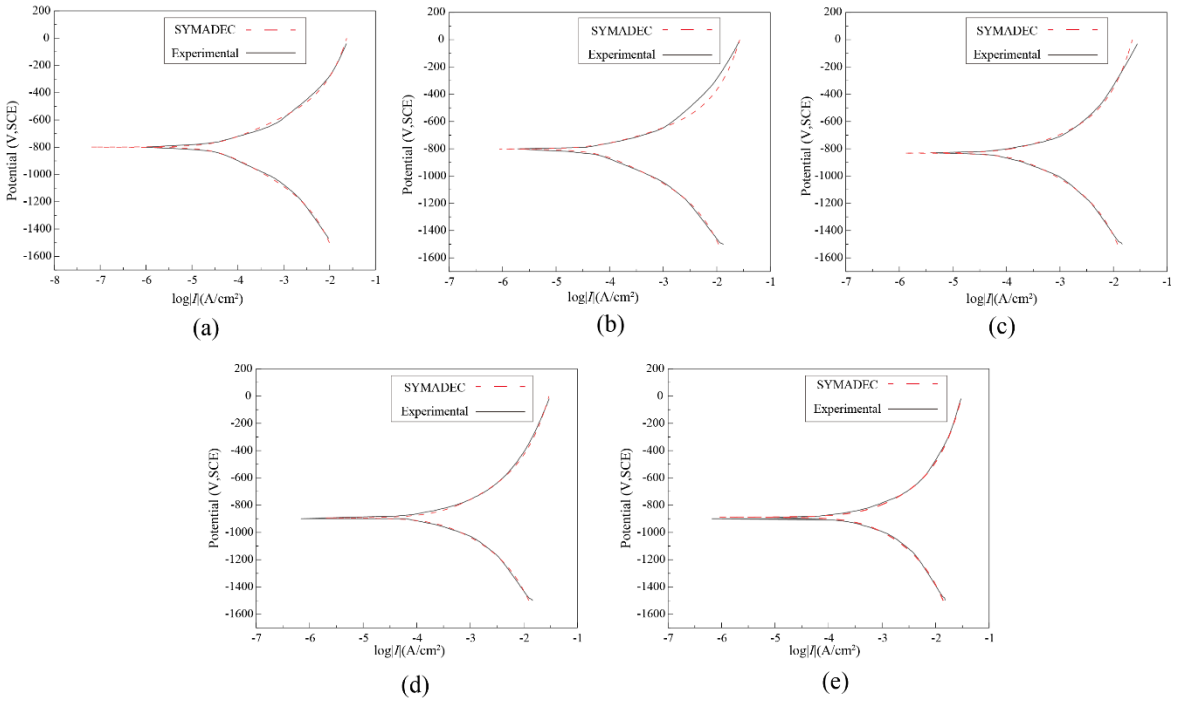

Figure 6. The fitting results of SYMADEC for Case I (a)20A/m^2 (b)50A/m^2 (c)100A/m^2 (d)200 A/m^2 (e)400A/m^2

The results obtained with SYMADEC match well with the experimental polarization curves (Fig. 6). Fig. 7 indicates that the corrosion at E_{corr} was mainly driven by oxygen reduction, and it took place under activation control. Moreover, the results (Table 10) are quite consistent with the values reported in Ref. [15] . As shown in Fig. 8, the values of I_{corr} evaluated via SYMADEC are in linear relation with the results of Ref. [15]. Therefore, SYMADEC is accurate way in evaluate the kinetics parameters from the polarization curves.

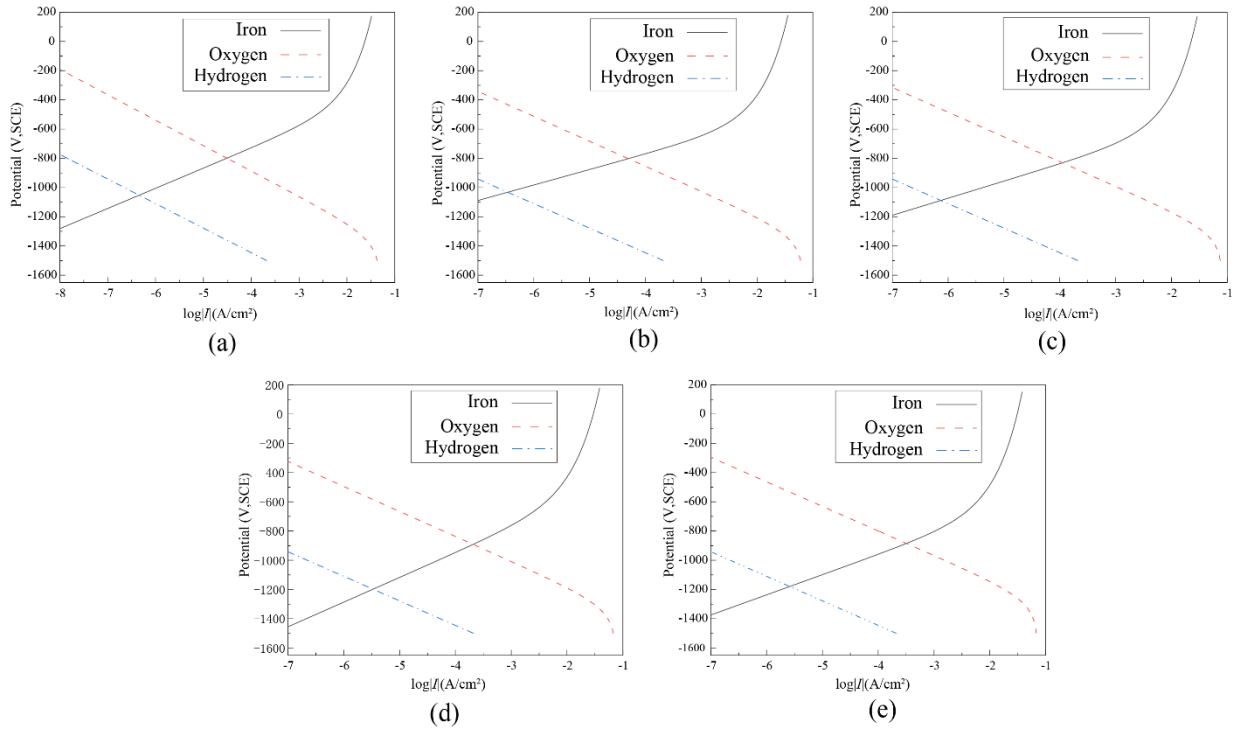

Figure 7. The deconstructed anodic and cathodic components of SYMADEC for Case I (a)20A/m^2 (b)50A/m^2 (c)100A/m^2 (d)200 A/m^2 (e)400A/m^2

Table 10. The results of SYMADEC for Case I

i_{AC} (A/m^2)	E_{corr} (mV,SCE)	I_{corr} (A/cm^2)	β_a (mV/decade)	β_c (mV/decade)	β_a /β_c
20	-799	3.04×10^{-5}	138	174	0.79
50	-803	4.60×10^{-5}	106	171	0.62
100	-833	9.08×10^{-5}	117	169	0.69
200	-895	1.86×10^{-5}	169	171	0.99
400	-891	2.37×10^{-5}	138	168	0.82

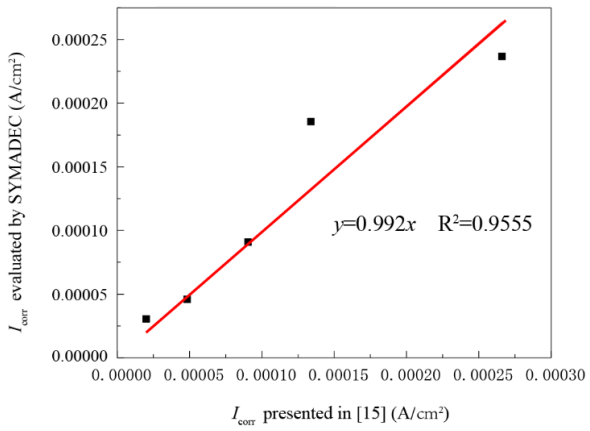

Figure 8. I_{corr} of Case I evaluated by SYMADEC

SYMADEC also was used to fit the polarization curves of Case II. The fit is presented in Fig. 9 and the estimated kinetics parameters are listed in Table 11. Despite the cathodic branches of the polarization curves were measured under the diffusion control and they are more complicated than those in Case I, which were obtained under the activation control, and the vibrations introduced by the AC are obviously present, the fitted curves almost coincide with the experimental ones. Hence, SYMADEC is more robust and suitable for the analyses of the polarization curves than other methods when AC is applied. The deconstructed results indicate that the corrosion at E_{corr} was mainly driven by oxygen reduction, which was under completed diffusion control. Moreover, as the potential shifts to more negative values than E_{corr}, the role of the hydrogen evolution reaction in the total cathodic process becomes more important. In the fitting process of SYMADEC, it was found that the adjustment of β_c in a large range almost has no effect on the shape of the calculated curves. This may be due to the fact that the cathodic polarization was under intensive diffusion control and the limiting current density dominated the polarization process causing β_c to become less meaningful. Therefore, β_c is not listed in Table11.

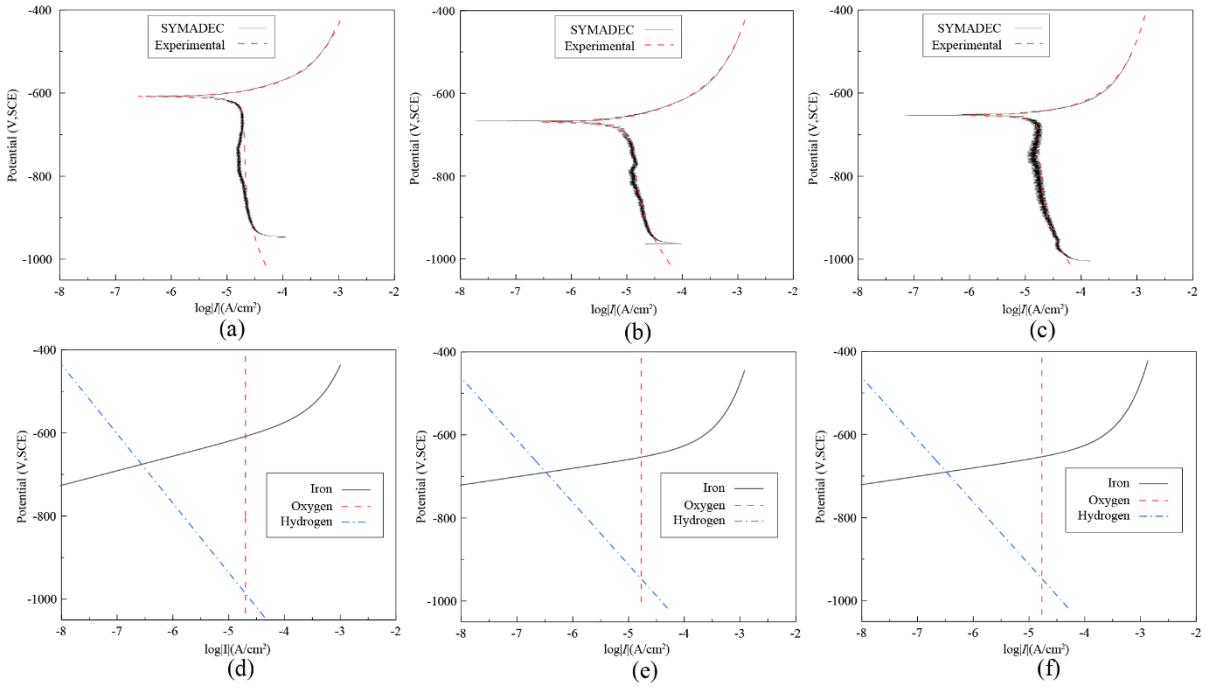

Figure 9. The fitting results and deconstructed anodic and cathodic components of SYMADEC for Case II (a) (d)20A/m^2 (b)(e)30A/m^2 (c)(f)50A/m^2

Table 11. The results of SYMADEC for Case II

i_{AC} (A/m^2)	E_{corr} (mV,SCE)	I_{corr} (A/cm^2)	β_a (mV/decade)
20	-610	1.57×10^{-5}	35
30	-671	1.21×10^{-5}	46
50	-657	1.72×10^{-5}	20

3.3 The effectiveness of SYMADEC

From the results of Case I and Case II, it can be roughly concluded that SYMADEC has advantages in dealing with complicated polarization curves under the effect of AC, due not only to that it is robust but also to that it can reveal more information about the anodic and cathodic reactions by deconstructing the curves. Despite the results of SYMADEC are remarkable, more polarization data still need to be studied to furtherly validate its effectiveness. Therefore, two more sets of polarization curves subject to AC that have been presented in different published literatures were also treated by SYMADEC and the results were compared with their originals. One set consists the polarization curves of X60 pipeline steel immerged in a simulated soil solution under the condition of AC densities of 50 and 100A/m^2. [37] The other involves the polarization curves of X70 pipeline steel tested in 3.5wt% NaCl solution under the condition of AC densities of 30 and 100A/m^2. [38] The fitting results and deconstructed anodic and cathodic components of SYMADEC are shown in Fig. 10 and Fig. 11. The estimated kinetics parameters are listed in Table 12 and Table 13.

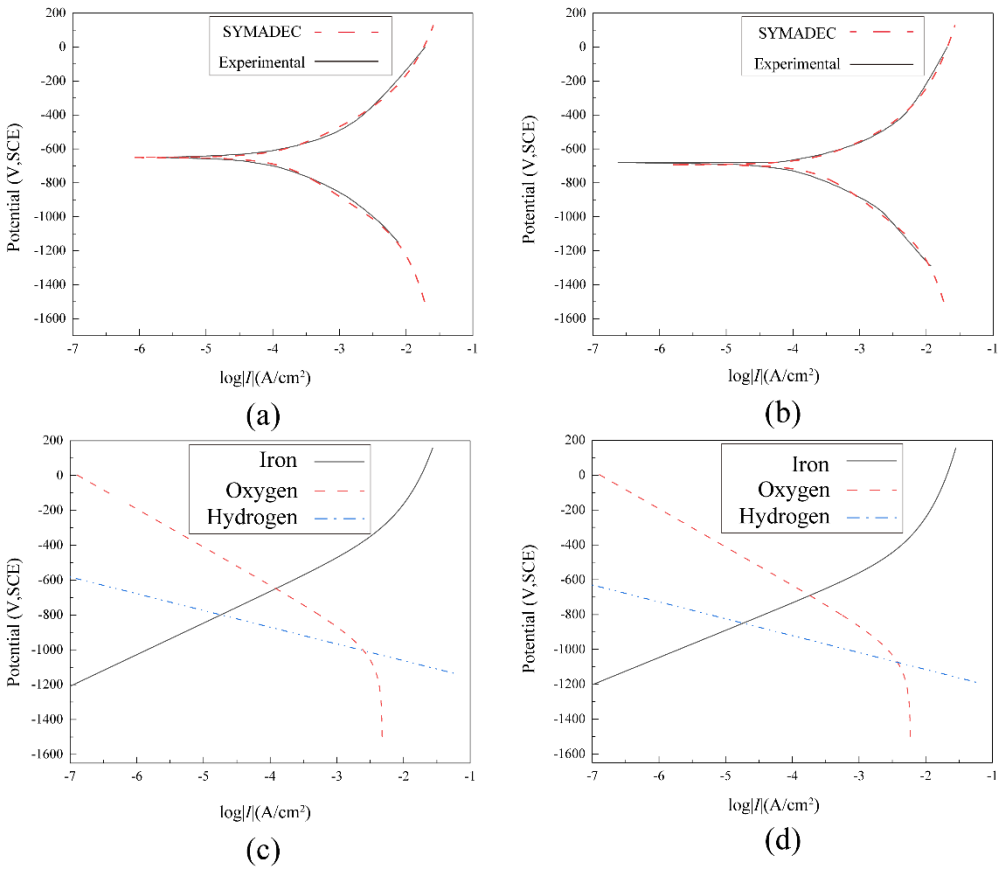

Figure 10. The fitting results and deconstructed anodic and cathodic components of SYMADEC for Ref. [37] (a) (c)50A/m^2 (b)(d)100A/m^2

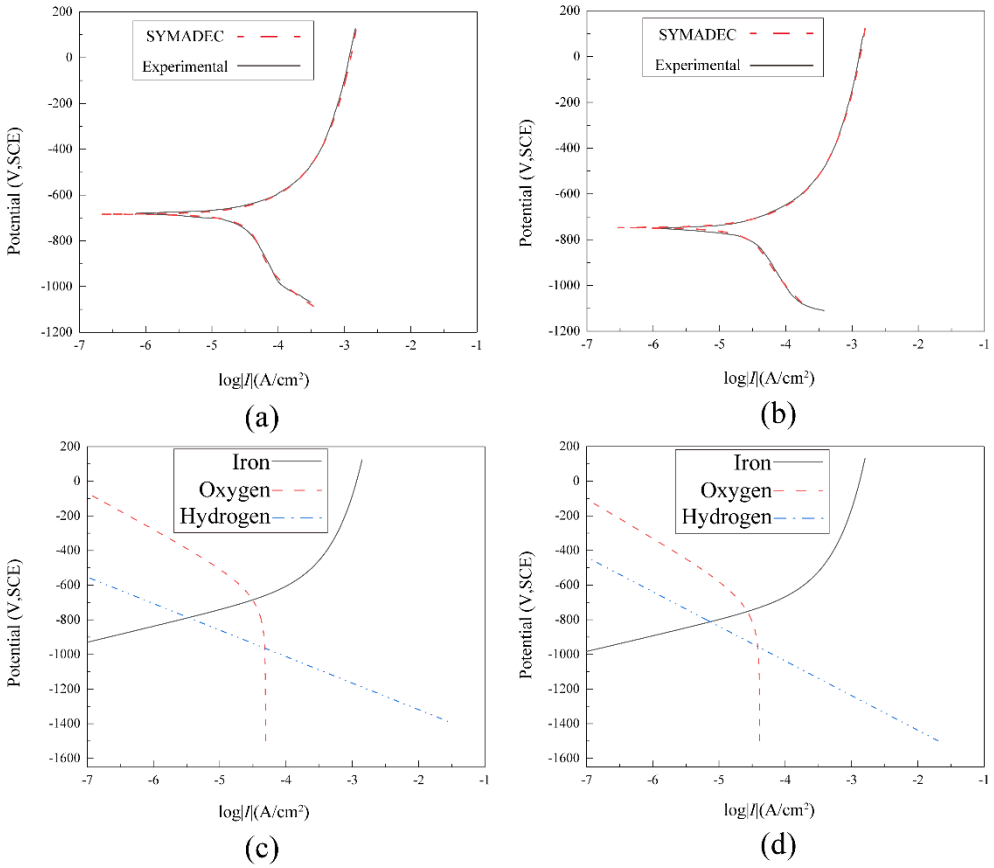

Figure 11. The fitting results and deconstructed anodic and cathodic components of SYMADEC for Ref. [38] (a) (c)30A/m^2 (b)(d)100A/m^2

As demonstrated in Fig. 10 and Fig. 11, the fitted curves almost coincide with the experimental ones. The deconstructed anodic and cathodic components show that the corrosion at E_{corr} was driven by oxygen reduction, which was under activation control in Fig. 10 and was under critical diffusion control in Fig. 11. The kinetics parameters presented in the literatures are quite different from that estimated by SYMADEC as shown in Table 12 and Table 13.

Table 12. The kinetics parameters of Ref. [37] and SYMADEC

	i_{AC} (A/m^2)	E_{corr} (mV,SCE)	I_{corr} (A/cm^2)	β_a (mV/decade)	β_c (mV/decade)	β_a /β_c
Ref. [37]	50	-657	5.90×10^{-5}	124	157	0.79
	100	-690	9.66×10^{-5}	145	191	0.76
SYMADEC	50	-649	1.31×10^{-4}	181	218	0.83
	100	-690	1.92×10^{-4}	156	219	0.71

Table 13. The kinetics parameters of Ref. [38] and SYMADEC

	i_{AC} (A/m^2)	E_{corr} (mV,SCE)	I_{corr} (A/cm^2)	β_a (mV/decade)	β_c (mV/decade)	β_a /β_c
Ref. [38]	30	-680	4.27×10^{-6}	296	552	0.54
	100	-747	4.43×10^{-6}	538	634	0.85
SYMADEC	30	-698	4.57×10^{-5}	92	210	0.44
	100	-751	5.49×10^{-5}	90	225	0.40

In order to demonstrate the difference between the shapes of the polarization curves in the presence of different AC densities, they are put together, as shown in Fig. 12. As demonstrated, the anodic branches of two polarization curves of X60 pipeline steel are near to each other, and the cathodic branches are almost overlapped. Similarly, both of the anodic and cathodic branches of two polarization curves of X70 pipeline steel are also overlapped to each other. The value of fitted kinetics parameters should approach to each other if the polarization curves are similar. Therefore, it can be inferred that β_c of the two polarization curves of X60 pipeline steel should be approximately equal, as well as the β_a and β_c of the two polarization curves of X70 pipeline steel. However, the results in the literatures are not consistent with this inference. For example, the β_a of X70 pipeline steel under the two AC densities are 296 and 538 mV/decade, presenting a huge difference.

Conversely, the results of SYMADEC are quite consistent with this inference, as the β_c of X60 pipeline steel under AC of 50A/m^2 is 218 mV/decade while under 100A/m^2 is 219 mV/decade, and the β_a of X70 pipeline steel under the two AC densities are 92 and 90 mV/decade, and β_c are 210 and 225 mV/decade. Hence, it can be concluded that the results of SYMADEC are reasonable.

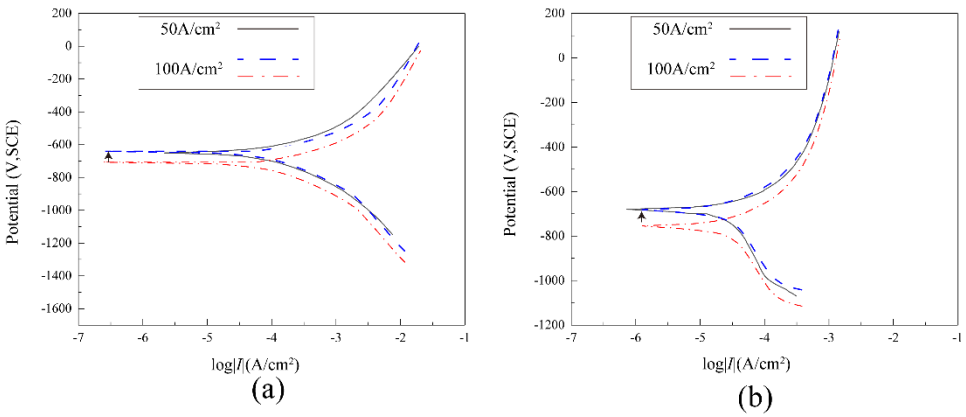

Figure 12. The comparation of different polarization curves (a) polarization curves of X60 pipeline steel in Ref. [37] (b) polarization curves of X70 pipeline steel in Ref. [38]

4. CONCLUSIONS

The polarization curves of the pipeline steels under the effect of the AC exhibit no Tafel region and these challenges the determination of the kinetics parameters from the experimental data. Three

methods, the Tafel extrapolation, the non-linear curve fitting method, and the SYMADEC method, were used to treat the polarization curves.

The Tafel exploration is easy to implement, but its results depend on the selection of the linear portions of the curves. Therefore, when the polarization curves do not present a liner trend, the use of this method may induce errors in the calculation.

The non-linear curve fitting method is applicable in theory, however, in practice it easily fails to provide accurate results due to the noise or errors contained in the experimental data.

SYMADEC is a powerful method, which can be used to treat polarization curves not presenting the Tafel region. Moreover, its results can be deconstructed into the anodic and cathodic components revealing more kinetics information about the electrode process.

Therefore, in the study of the AC corrosion behaviors, the treatment of the polarization curves is important and should be carefully performed to obtain accurate kinetics parameters. For samples, which do not exhibit a Tafel region, the use of SYMADEC is recommended.

References

1. R. T. Loto, *J. Mater. Res. Technol*., 8 (2018) 623.
2. S. L. Assis, S. Wolynec and I. Costa, *Electrochim. Acta,* 51 (2006) 1815.
3. M. I. Abdulsalam, *Corros. Sci.*, 138 (2018) 307.
4. A. G. Dos Santos Jr, L. V. Biehl and L. M. Antonini, *Mater. Corros*., 68 (2017) 824.
5. H. Luo, X. Z. Wang, C. F. Dong, K. Xiao and X. G. Li, *Corros. Sci*., 124 (2017) 178.
6. Y. Zuo, L. Yang, Y. J. Tan, Y. S. Wang and J. M. Zhao, *Corros. Sci.*, 120 (2017) 99.
7. D. T. Chin and T. W. Fu, *Corros.*, 35 (1979) 514.
8. D. T. Chin and S. Venkatesh, *J. Electrochem. Soc.*, 126 (1979) 1908.
9. D. T. Chin and P. Sachdev, *J. Electrochem. Soc.*, 130 (1983) 1714.
10. T. C. Tan and D. T. Chin, *J. Electrochem. Soc*., 132 (1985) 766.
11. J. L. Wendt and D. T. Chin, *Corros. Sci.*, 25 (1985) 889.
12. J. Wendt and D. Chin, *Corros. Sci*., 25 (1985) 901.
13. T. C. Tan and D. T. Chin, *J. Appl. Electrochem.*, 18 (1988) 831.
14. S. Goidanich, L. Lazzari and M. Ormellese, *Corros. Sci*., 52 (2010) 491.
15. L. Y. Xu, X. Su, Z. X. Yin, Y. H. Tang and Y. F. Cheng, *Corros. Sci.*, 61 (2012) 215.
16. X. H. Wang, X. T. Song, Y. C. Chen, Z. Q. Wang and L. W. Zhang, *Int. J. Electrochem. Sci*., 13 (2018) 6436.
17. H. J. Flitt and D. P. Schweinsberg, *Corros. Sci*., 47 (2005) 3034.
18. R. G. Kelly, J. R. Scully, D. Shoesmith and R. G. Buchheit, Electrochemical techniques in corrosion science and engineering, CRC Press, (2002), USA.
19. I. Qamar and S. W. Husain, *Corros. Eng., Sci. Technol.*, 25 (1990) 202.
20. G. Rocchini, *Corros. Sci*., 37 (1995) 987.
21. H. J. Flitt and D. P. Schweinsberg, *Corros. Sci*., 47 (2005) 2125.
22. F. Mansfeld, *Corros. Sci.*, 47 (2005) 3178.
23. E. McCafferty, *Corros. Sci.*, 47 (2005) 3202.
24. K. V. Rybalka, L. A. Beketaeva and A. D. Davydov, *Russ. J. Electrochem*., 50 (2014) 108.
25. L. Stephens, S. C. Perry, S. M. Gateman, R. Lacasse, R. Schulz and J. Mauzeroll, *J. Electrochem. Soc.*, 164 (2017) 3576.
26. R. W. Bosch and W. F. Bogaerts, *Corros. Sci*., 40 (1998) 323.
27. R. Zhang, P. R. Vairavanathan and S. B. Lalvani, *Corros. Sci.*, 50 (2008) 1664.

28. Z. T. Jiang, Y. X. Du, M. X. Lu, Y. N. Zhang, D. Z. Tang and L. Dong, *Corros. Sci*., 81 (2014) 1.
29. I. Ibrahim, B. Tribollet, H. Takenouti and M. Meyer, *J. Braz. Chem. Soc*., 26 (2015) 196.
30. D. Kuang and Y. F. Cheng, *Corros. Eng., Sci. Technol*., 52 (2017) 22.
31. C. Wagner and W. Traud, *Z. Elektrochem*, 44 (1938) 391.
32. S. Barnartt, *Electrochim. Acta*, 15 (1970) 1313.
33. J. Jankowski and R. Juchniewicz, *Corros. Sci*., 20 (1980) 841.
34. L. M. Rivera Grau, M. Casales, I. Regla, D. M. Ortega Toledo, J. A. Ascencio Gutierrez, J. Porcayo Calderon and L. Martinez Gomez, *Int. J. Electrochem. Sci*., 8 (2013) 2491.
35. M. Alfaro, *Alexandria Eng. J*., 53 (2014) 977.
36. D. Jones, *Corros.*, 34 (1978) 428.
37. Y. B. Guo, C. Liu, D. G. Wang and S. H. Liu, *Pet. Sci.,* 12 (2015) 316.
38. Y. C. Li, C. Xu, R. H. Zhang, Q. Liu, X. H. Wang and Y. C. Chen, *Int. J. Electrochem. Sci*., 12 (2017) 1829.